JOURNAL OF MATERIALS SCIENCE **34** (1999) 3859–3866

Preparation, structure and properties of uniaxially oriented polyethylene-silver nanocomposites

Y. DIRIX, C. BASTIAANSEN, W. CASERI, P. SMITH
Department of Materials, ETH Zürich, CH-8092 Zürich, Switzerland
E-mail: wcaseri@ifp.mat.ethz.ch

Uniaxially oriented composites of high-density polyethylene and silver nanoparticles were prepared using solution-casting, melt-extrusion and solid-state drawing techniques. The absorption spectrum in the visible wavelength range of the drawn nanocomposites was observed to strongly depend on the polarisation direction of the incident light. For instance, the nanocomposites appear bright yellow or red when the vibration direction of linearly polarised light is perpendicular or parallel, respectively, to the drawing axis. The optical anisotropy of the drawn nanocomposites originates from uniaxially oriented, pearl-necklace type of arrays of nanoparticles of high aspect ratios. The absorption spectrum of the nanocomposites can be shifted to higher wavelengths using appropriate annealing procedures. The annealing results in an increased size of the primary silver particles, due to Ostwald ripening, and consequently a range of polarisation-dependent colours can be generated in the drawn nanocomposites.

1. Introduction

The synthesis and properties of a large range of inorganic nanoparticles with a typical size in the range of 1–100 nm was extensively investigated in the past, and a variety of routes were discovered to produce such particles with a strongly bound organic surface layer [1–5]. Typically, an organic surface layer is used onto these nanoparticles to lower the surface energy, to prevent particle aggregation into larger structures or to disperse the particles in, for instance, organic solvents. The above described advances have opened the possibility to produce composites based on synthetic polymers containing well-dispersed ceramic or metallic nanoparticles [6, 7]. Large-scale aggregation of the nanoparticles may also be avoided with polymer-stabilized particles using appropriate materials and processing routes. With certain methods, transparent materials can be obtained, due to the small size of the nanoparticles which prevents excessive light scattering [8–11]. Apart from a high transparency, such nanocomposites also possess a variety of other potentially useful properties. For instance, it has been shown previously that polymer-based nanocomposites containing well-dispersed inorganic particles can exhibit semiconducting properties [12, 13], quantum dot effects [14], non-linear optical properties [15, 16] and an extremely low [17], or high [18] refractive index.

Here, experimental results are presented concerning the manufacturing, structure and properties of mechanically robust, flexible, thin polymeric films containing metallic nanoparticles with an organic surface layer, that exhibit interesting optical properties; a brief synopsis of which was previously published [19]. In contrast to the above described studies, here it is attempted to generate anisotropy in the films via the classical orientation technique solid-state drawing. More specifically, it is attempted to generate structural anisotropy in both the continuous phase (i.e. synthetic polymer) and in the dispersed phase (metallic nanoparticles), and the influence of the anisotropy on the optical characteristics in the visible wavelength range of the films is investigated. It is shown that rather unusual, potentially useful, anisotropic optical phenomena can be generated in these films in a well-controlled manner.

2. Experimental

2.1. Synthesis of the nanoparticles

The synthesis of colloidal silver particles with a surface layer of dodecanethiol was performed according to (somewhat modified) methods described in the literature [3–5]; Silver trifluoromethanesulfonate (CF_3SO_3Ag, $9 \cdot 10^{-4}$ mol), tetraoctylammonium bromide ($[C_8H_{17}]_4NBr$, $4 \cdot 10^{-3}$ mol) and 1-dodecanethiol ($C_{12}H_{25}SH$, $1.8 \cdot 10^{-3}$ mol) were dissolved in 80 ml toluene. A freshly prepared aqueous sodiumborohydride solution ($1 \cdot 10^{-2}$ mol in 25 ml distilled water) was slowly added under vigorous stirring, and the solution was stirred for another hour. The organic layer was separated, and the mixture was concentrated by solvent evaporation to a volume of approximately 5 ml. Then 500 ml ethanol was added at $-20\,^{\circ}C$. After sedimentation of the particles, the mixture was decanted, and the residue was again treated with 500 ml ethanol at $-20\,^{\circ}C$. Finally the particles were dried for 12 h at room temperature and reduced pressure (ca. 10 mbar).

2.2. Preparation of the nanocomposites

Solution-cast films were prepared by dispersing various amounts of the metal nanoparticles (10–100 mg) in 50 ml of *p*-xylene under stirring at room temperature in an ultrasonic bath (Branson 2210, 47 kHz). High-density polyethylene (0.5 g, Hostalen Gur 7225 P, $\overline{M}_w = 400$ kg/mol) was added and the dispersion was degassed at ca. 10 mbar for 30 min. The mixture was heated to 130 °C and stirred for 15 min until a homogeneous, dark brown liquid mixture was obtained. These mixtures were cast, quenched to room temperature and dried overnight at ambient conditions. After evaporation of the solvent, the films were compression moulded for 15 min at 180 °C. Some of the polyethylene/silver nanocomposites were annealed at 180 °C for 15 h. Melt-processed nanocomposites were made on a recycling, corotating twin-screw mini-extruder (DACA Instruments). A 2% w/w HDPE/silver nanoparticle blend was mixed for 10 min at 180 °C. The extrudates were subsequently compression moulded at 180 °C. All compression moulded, melt-crystallised films were finally drawn on a hot stage at 120 °C. The draw ratio was determined from the displacement of ink marks.

2.3. Characterization

Thermogravimetric analysis (TGA) and differential scanning calorimetry (DSC) were performed with, respectively, a Netzsch TG 209 thermogravimetrical analyser and with a Netzsch DSC 200. The samples (ca. 10 mg) were heated under a nitrogen flow of a heating rate of 10 °C/min.

Transmission electron microscopy (TEM) was performed using a Philips EM 301 electron microscope operating at an acceleration voltage of 80 kV. A drop of the toluene reaction mixture containing the colloidal metal particles was placed onto a carbon film supported by a copper grid. After evaporation of the toluene, the samples were inserted into the electron microscope. The morphology of both the undrawn and the drawn nanocomposite was also investigated with TEM. The undrawn nanocomposites were cut at low temperatures (−80 °C) using a diamond knife and coupes were collected on a copper grid. The drawn films were split into thin filaments which were placed on a copper grid. These filaments were sputtered with a carbon layer to reduce electron-beam damage during TEM.

Small-angle X-ray scattering (SAXS) patterns were obtained with a Kiessig camera, using Ni-filtered CuK_α-radiation generated by a Seifert ISO-Debeyeflex 2002 generator operating at 35 kV and 30 mA. The sample to film distance was 200 mm. X-ray patterns were recorded of the silver nanoparticles, and the undrawn and drawn nanocomposite films.

UV-Vis spectroscopy was performed using a Perkin Elmer Lambda 900 double beam spectrometer. Surface-coated metal nanoparticles were dispersed in xylene (1 mg/10 ml), and UV-Vis spectra were recorded in the wavelength range from 350 to 800 nm. Undrawn and drawn nanocomposites (4% w/w nanoparticles) were sandwiched between two quartz glass slides and coated with silicon oil to reduce light scattering at the film surface [20]. Absorption spectra in non-polarised light were recorded by placing a depolariser in the measuring and reference beam. Polarised UV-Vis spectra of the drawn nanocomposite were measured using motor driven Glan-Thomson prisms. Spectra were obtained at various angels (φ) between the polarisation direction of the incident light and the drawing direction of the films.

Photographs of different samples were taken at a low magnification (4×) using a Leica MS5 polarising microscope.

3. Results

3.1. Silver nanoparticles

According to the procedure detailed above, colloidal metal particles were obtained which are coated with an organic dodecanethiol layer. The nanoparticles can be re-dispersed in common organic solvents such as toluene or xylene. Transmission electron microscopy (TEM) shows that the particles were of a relatively narrow size distribution and had an average size of the primary particles of approximately 4.5 nm (Fig. 1a and b).

In Fig. 2, DSC thermograms are shown of the metallic nanoparticles as well as pristine dodecanethiol.

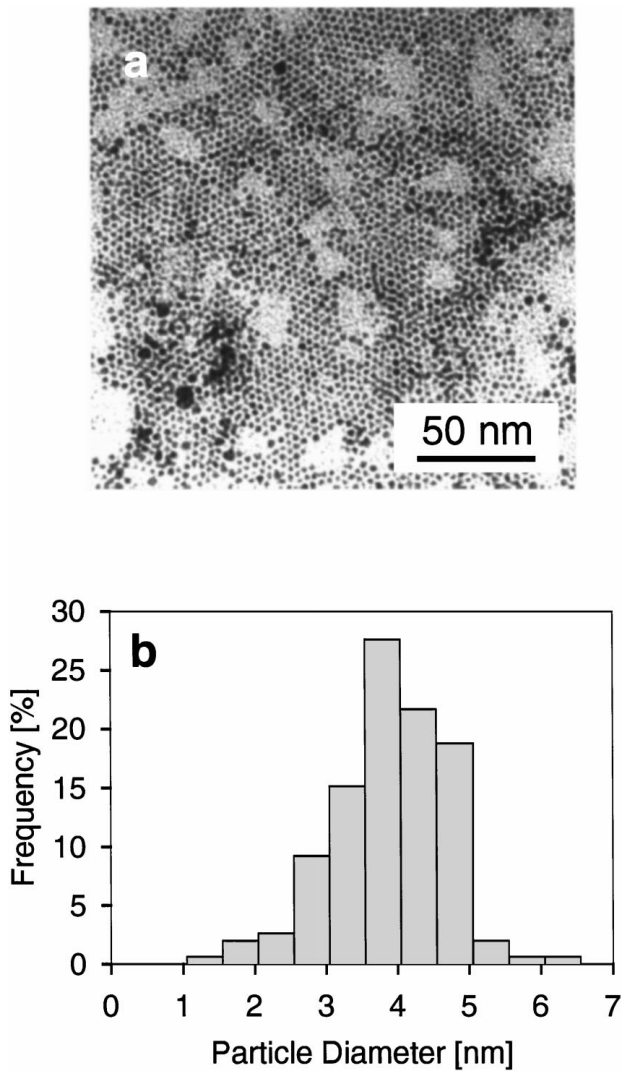

Figure 1 Transmission electron microscopy (TEM) micrograph of: (a) the silver nanoparticles, and (b) their size distribution.

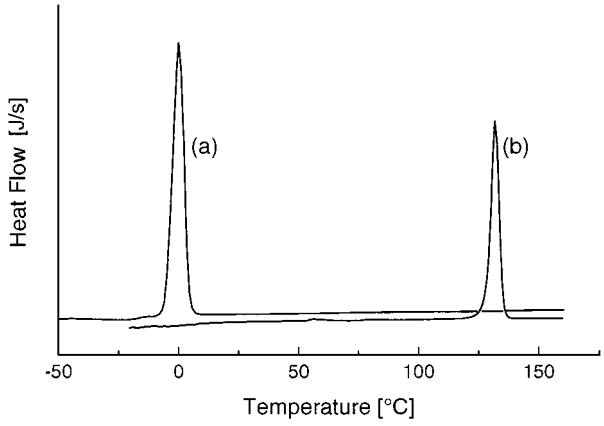

Figure 2 Differential scanning calorimetry (DSC) thermograms of: (a) pure dodecanethiol, and (b) dodecanethiol-coated silver nanoparticles.

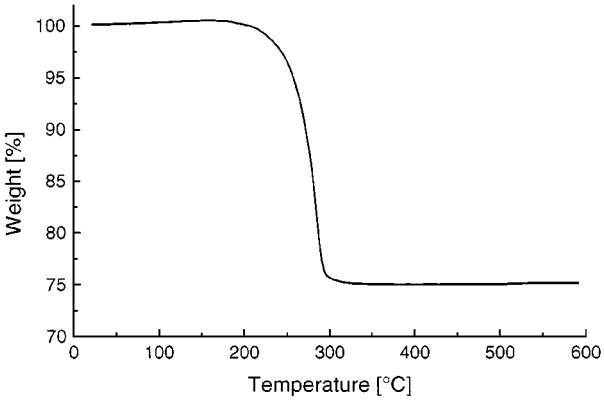

Figure 3 Thermogravimetric analysis (TGA) measurement of dodecanethiol-coated silver nanoparticles.

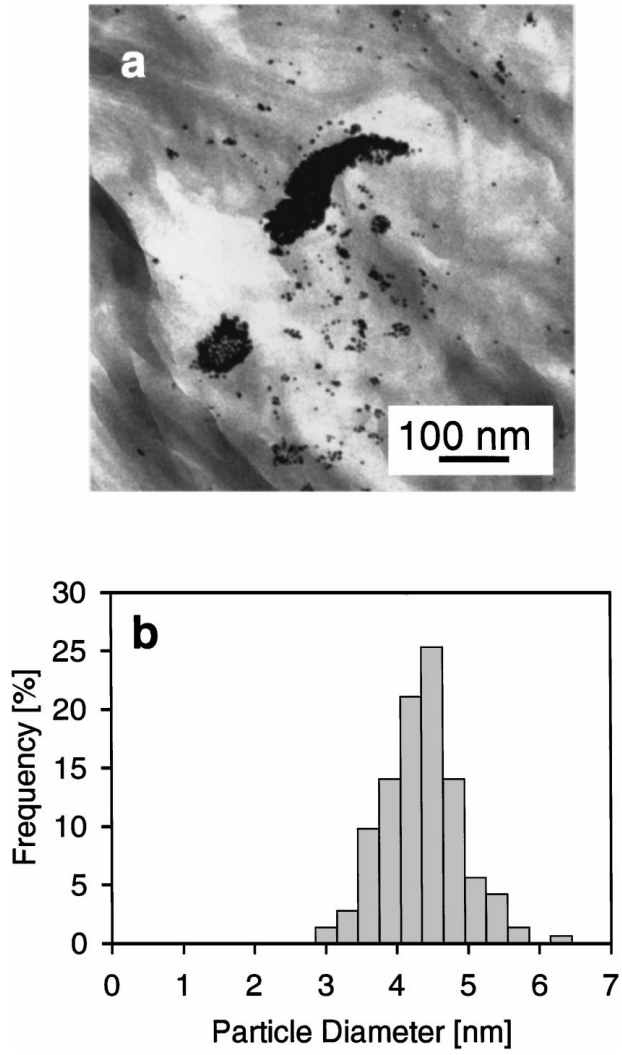

Figure 4 (a) TEM micrograph of: undrawn (isotropic) polyethylene/silver nanocomposites containing 4% w/w particles, and (b) their size distribution.

Interestingly, the dodecanethiol layer on the silver nanoparticles possesses a substantially higher melting temperature ($T_m = 131\,^{\circ}C$) compared to that of pure dodecanethiol ($T_m = 1\,^{\circ}C$), which, probably, originates from entropic effects related to the chemical anchoring of the dodecanethiol to the silver surface.

The thermal stability of the dodecanethiol layer on the silver particles was examined with thermogravimetric analysis (TGA, Fig. 3). Virtually no weight loss was observed below about 200 °C in a nitrogen atmosphere which indicates that the particles possess an excellent stability at elevated temperatures which is relevant, of course, for further processing. The silver content of the particles was determined from the residual weight fraction of the particles after prolonged heating at 600 °C, assuming that the remainder consists principally of elemental silver. A silver weight fraction of 75% w/w was measured for the nanoparticles, which corresponds to a silver volume fraction of approximately 22% v/v.

3.2. Polyethylene-silver nanocomposites

TEM micrographs of the undrawn nanocomposite (Fig. 4a) reveal that the silver particles are agglomerated, to a certain extent, in the polymer matrix. The individual silver nanoparticles in the aggregates can readily be distinguished in these micrographs. It was found that the primary particle size and size distribution are virtually identical prior to and after manufacturing of the films (cf. Figs 1b and 4b). The melt-crystallized nanocomposites were drawn on a hot stage at 120 °C to a draw ratio of 15. In the drawn samples, arrays of nanoparticles are observed which are aligned in the drawing direction (Fig. 5). The TEM micrographs illustrate the presence of pearl-necklace arrays of nanoparticles that possess a rather high aspect ratio (>20) and a typical width of 1 to 2 particle diameters. Evidently, the aggregates of silver particles in the undrawn films (Fig. 4a) rearrange into these pearl-necklace type arrays during solid-state drawing of the nanocomposites (Fig. 5).

The SAXS pattern of the as-synthesised particles is shown in Fig. 6a. An isotropic pattern is obtained with reflection rings at a characteristic d-spacing of 3.54 nm, suggesting that the particles are regularly packed. This might be due to cocrystallisation of the alkyl chains of different particles which would imply that the pristine particles are partially aggregated. The SAXS pattern of the undrawn polyethylene/silver nanocomposite is essentially identical to that of the particles alone (Fig. 6b, d-spacing = 3.46 nm) which means that the aggregated, and regularly-packed particle structure

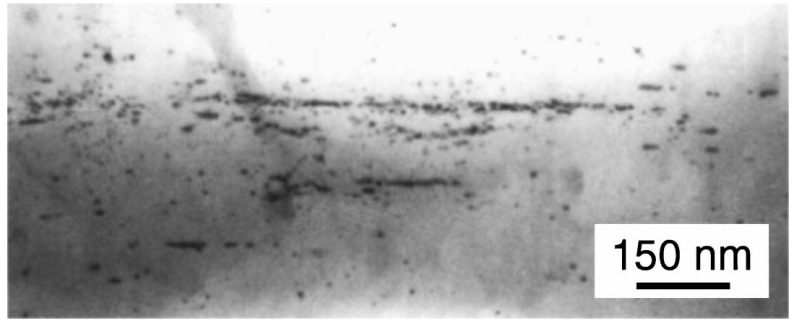

Figure 5 TEM micrograph of drawn (oriented, draw ratio = 15) polyethylene/silver nanocomposites containing 4% w/w particles.

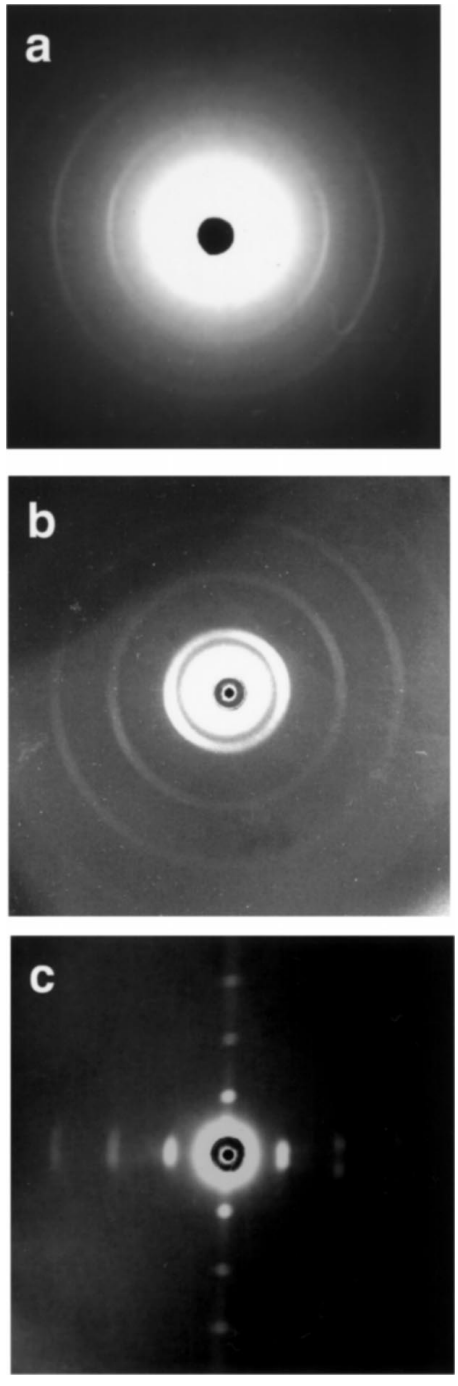

Figure 6 Small angle X-ray (SAXS) patterns of: (a) dodecanethiol-coated silver nanoparticles, (b) isotropic polyethylene/silver nanocomposites containing 4% w/w particles, and (c) oriented (draw ratio = 15) polyethylene/silver nanocomposites containing 4% w/w particles.

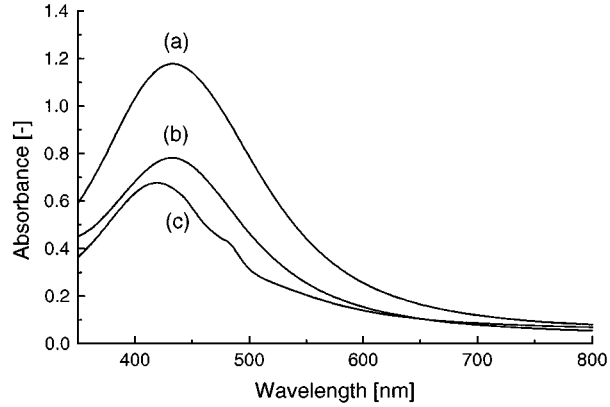

Figure 7 UV-Vis absorption spectra of silver nanoparticles in unpolarised light of: (a) dispersion in xylene, (b) undrawn nanocomposite (4% w/w particles), and (c) drawn nanocomposite (draw ratio = 15).

is still present in the isotropic nanocomposite. After drawing, a 2-dimensional pattern is observed with reflection spots at a spacing of 3.43 nm (Fig. 6c). Evidently, the aggregated silver particles are rearranged into surprisingly highly ordered pearl-necklace chains during solid-state deformation of the films.

The optical properties of the nanoparticles in a reference xylene dispersion, in an undrawn nanocomposite and a drawn nanocomposite were investigated using UV-Vis spectroscopy. The absorption spectrum of the particles dispersed in xylene is virtually identical to the spectrum of the undrawn nanocomposite containing 4% nanoparticles (Fig. 7a and b). This experimental observation indicates that the degree of aggregation of the nanoparticles in the dispersion and in the undrawn nanocomposite are comparable, since shifts in the absorption maximum are extremely sensitive to the state of aggregation of the metal particles [23]. Hence, we conclude that the aggregates of silver particles, which are observed for the undrawn nanocomposite with TEM (Fig. 4a) and identified with SAXS (Fig. 6b), are already present in the xylene dispersion prior to film manufacturing; and it appears that the state of aggregation is preserved in subsequent processing-steps.

It is evident from the data in Fig. 7 that the absorption spectrum of the nanocomposites changes significantly upon solid-state drawing. For instance, a pronounced shoulder is observed in the absorption spectrum at a wavelength of approximately 490 nm (Fig. 7c).

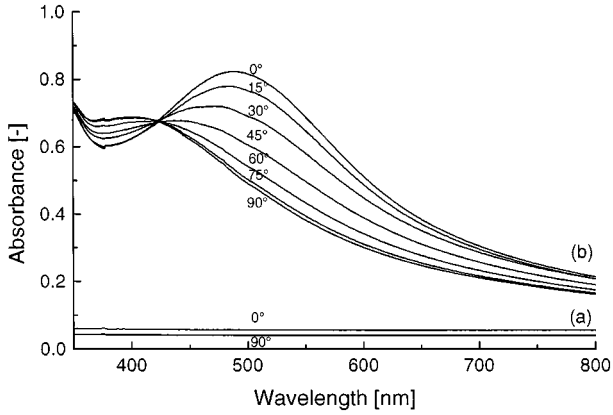

Figure 8 Absorption spectra in linearly polarised light of: (a) drawn polyethylene films (draw ratio = 15), and (b) oriented silver/polyethylene nanocomposites (4% w/w particles) as a function of the angle (φ) between the polarisation direction and the drawing direction.

Absorption spectra recorded with linearly polarised light of a drawn polyethylene film containing 4% w/w silver nanoparticles are shown in Fig. 8. The absorption spectra of the films without nanoparticles are included for reference purposes. Clearly, the absorption of the latter films is low (<0.06) and virtually constant in the entire visible wavelength range. The absorption spectra of the drawn nanocomposites exhibit a strong dependence on the angle φ between the polarisation direction of the incident light and the drawing direction of the films. Light vibrating parallel to the drawing axis ($\varphi = 0^\circ$) is absorbed at higher wavelengths with a maximum absorption at 489 nm, while light vibrating perpendicular to this axis ($\varphi = 90^\circ$) is absorbed at lower wavelengths with a maximum at 398 nm. An isosbestic point is observed at 425 nm.

In Fig. 9a and b, photographs are shown of a drawn silver/HDPE nanocomposite, taken in linearly polarised light. The colour of the films depends strongly on the polarisation direction of light, in accordance with the UV-Vis measurements. The films exhibit bright colours and appear red or yellow, dependent on the polarisation direction of incident light.

The wavelengths of the absorption maxima in parallel ($\varphi = 0^\circ$) and perpendicular polarised light ($\varphi = 90^\circ$), respectively, are depicted in Fig. 10 as a function of the draw ratio of the films. The wavelength shift already occurs at low (<10) draw ratios and remains at a constant level of approximately 90 nm. Data are presented for nanocomposites produced by either the solution-casting technique or by melt-extrusion in Fig. 10. It can be observed that the wavelength shift virtually is independent on the production procedure of the films.

A few attempts were performed to generate other, polarisation-direction dependent, colours in the drawn nanocomposites. For instance, an undrawn polyethylene film containing silver nanoparticles was annealed at 180 °C for 15 h and TEM micrographs of the annealed films were recorded (Fig. 11). The silver nanoparticles

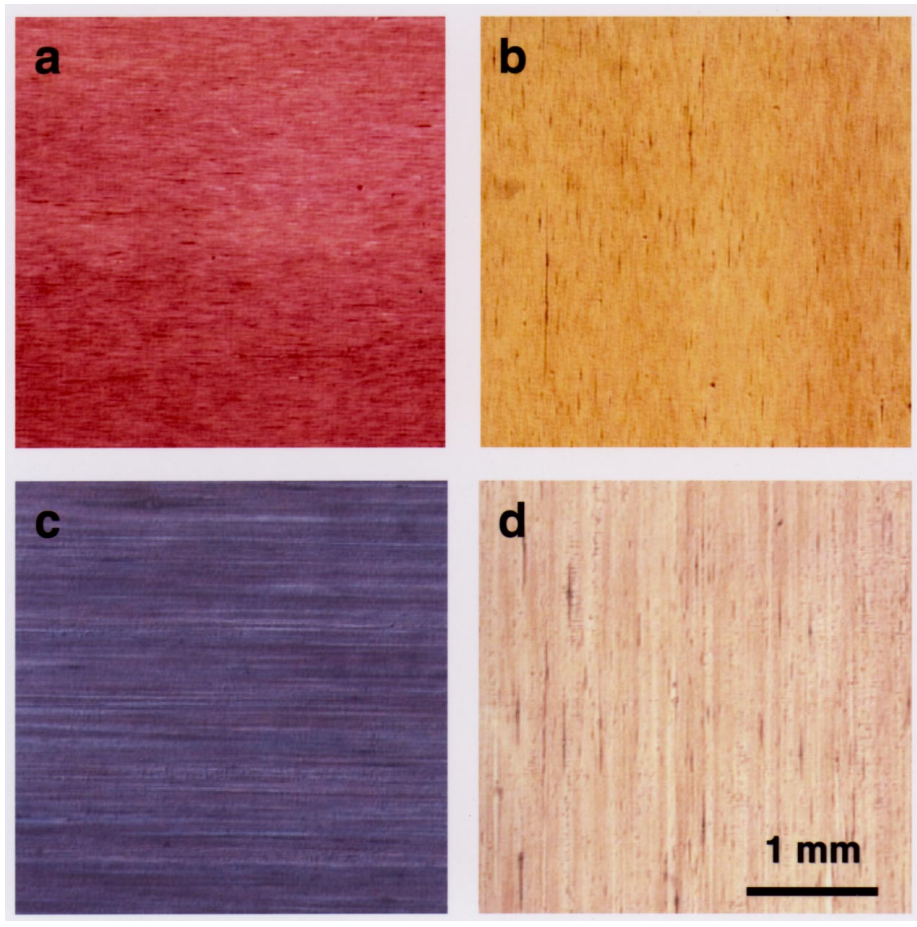

Figure 9 Photographs taken in polarised light of drawn silver/polyethylene nanocomposites (draw ratio = 15). Nanocomposite compression moulded at 180 °C for 15 min prior to drawing in: (a) parallel, and (b) perpendicular polarised light. Nanocomposite annealed for 15 h at 180 °C prior to drawing in (c) parallel, and (d) perpendicular polarised light.

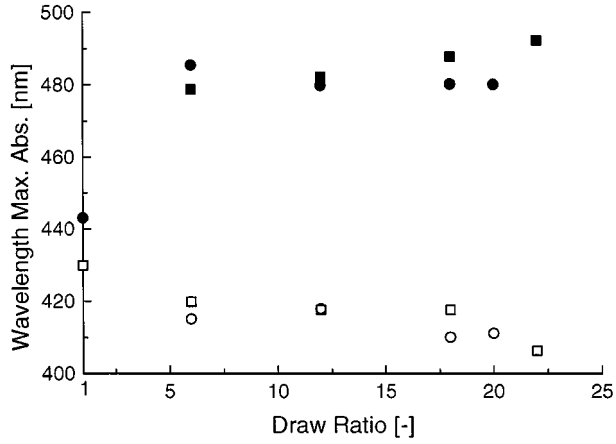

Figure 10 Absorption maxima as a function of the draw ratio of the polyethylene/silver nanocomposite films: solution-processed films in parallel polarised light (●) and perpendicular polarised light (○); melt-extrusion-processed films in parallel (■) and perpendicular polarised light (□).

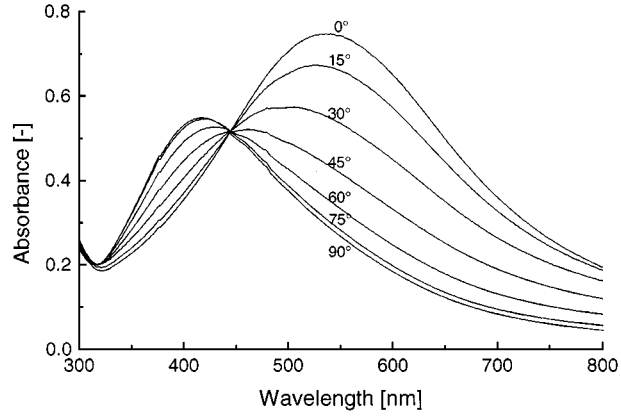

Figure 12 Absorption spectra in polarised light of a drawn (draw ratio = 15) silver/polyethylene nanocomposite film as a function of the angle (φ) between the polarisation and drawing direction. The polyethylene/silver film was annealed for 15 h at 180 °C before drawing.

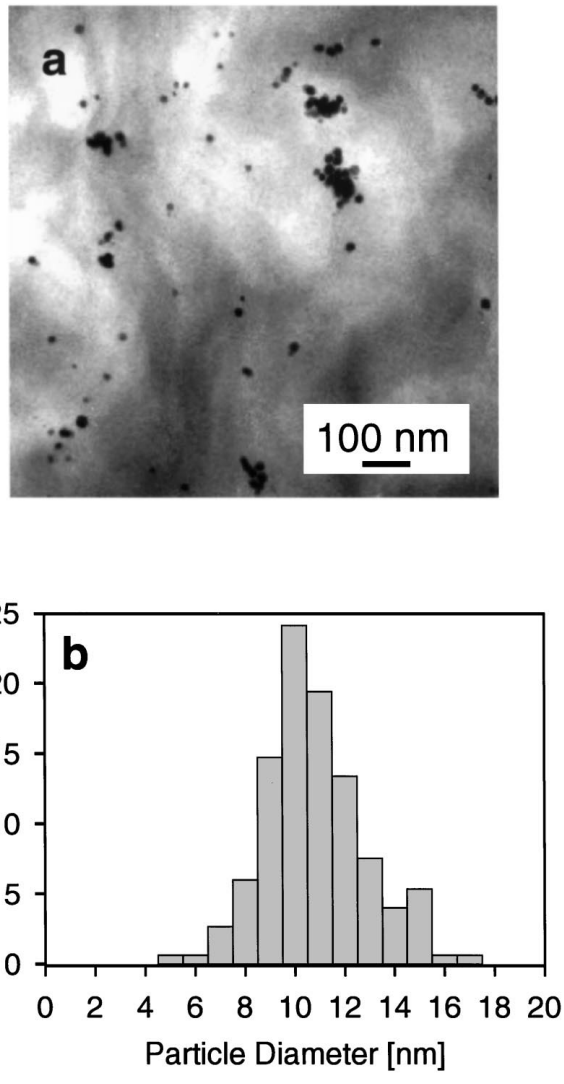

Figure 11 (a) TEM micrograph of: undrawn polyethylene/silver nanocomposite annealed for 15 h at 180 °C, and (b) the corresponding silver-particle size distribution.

remain slightly aggregated, but the size of the individual nanoparticles was found to increase from approximately 4.5 to 10 nm (compare Figs. 4b and 11b), presumably due to Ostwald ripening [21]. This increase in particle diameter, of course, also results in a wavelength shift in the absorption spectrum of the undrawn nanocomposites; i.e. the absorption maximum in unpolarised light increases from 435 to 463 nm.

The UV-Vis spectra of an annealed, drawn nanocomposite in linearly polarised light is shown in Fig. 12. In comparison with the non-annealed films, the absorption maxima are again shifted towards higher wavelengths (compare with Fig. 8). Of course, these shifts influence the colour of the films when observed in linearly polarised light (Fig. 9c and d). In this particular case, the colour changes from purple to yellow dependent on the polarisation direction of incident light.

4. Discussion

Extensive studies were performed in the past concerning the optical characteristics of dispersions of metal nanoparticles in liquids or in isotropic polymeric nanocomposites [21–24]. These studies showed that the absorption spectra of the nanoparticles depend on the particle size and its polydispersity, the degree of aggregation of the nanoparticles, the type of metal and the interaction of the nanoparticles with their environment. A variety of widely forgotten studies also exist that concern dichroism in oriented substrates, both natural-based [25–29] and synthetic polymers [30, 31] containing elemental metal nanoparticles. Already in this early work it was shown that the absorption spectrum of these anisotropic nanocomposites depends on the polarisation direction of incident light. Usually, these materials were produced by the *in situ* reduction of metal salts in the presence of preoriented substrates such as plant fibrils [25–29], stretched gelatine [26] or poly(vinylalcohol) [30, 31]. More recent studies used friction-deposited oriented poly(tetrafluoroethylene) layers for the oriented growth of metal nanoparticles [32–34]. The experimental routes used in these studies almost invariably resulted in the formation of large quantities of by-products in the materials, in experimental difficulties in obtaining large area flexible films, in a limited range of obtainable colours, or combinations thereof.

The present work explored new routes to prevent the above restrictions and to produce flexible, polymeric films which exhibit a polarisation dependent, and tunable colour. Here, it is shown that polymeric films containing slightly aggregated metallic nanoparticles can be produced and that these aggregates can, subsequently, be deformed into pearl-necklace types of arrays by solid-state drawing at temperatures below the melting temperature of the polymer. The formation of the pearl-necklace type of arrays results in films which, indeed, exhibit a strongly polarisation-direction dependent colour. In our method, the metallic nanoparticles are first synthesised and purified and, therefore, the presence of large quantities of by-products in the films is prevented. Also, we employed conventional processes for the processing of synthetic polymers which drastically facilitates the production of large area, flexible films.

The colour of the films in linearly polarised light can be varied, to a certain extent, by using appropriate annealing procedures. Of course, further colour tuning can be performed in several other ways, for instance, by the direct synthesis of larger silver particles or even by the synthesis of non-spherical particles with a predetermined aspect ratio, followed by the preparation and orientation of the nanocomposites.

In the previous studies concerning oriented systems with elemental metal particles, the colour shift was either attributed to the formation of oriented metallic needles or, comparable to our observations, attributed to a chain-like ordering of individual spherical metal particles. Recently, Lu *et al.* [34] studied the dichroism of surface-coated gold nanoparticles which were deposited onto oriented poly(tetrafluoroethylene) substrates. Only very weak dichroism was observed, although the thiol-coated gold particles were arranged in oriented arrays, which they attributed to the electrical isolation of the separate particles by the organic layer surrounding each particle. Strong dichroism was observed after removal of the surface coating of the particles and the polymer substrate by burning in a torch at 1700 °C. It was suggested that the observed optical phenomena originate from the formation of metallic needles during the heat treatment. In the present study, arrays of thiol-coated, electrically isolated, silver particles are produced in a polymer film and strong dichroism is nonetheless observed, suggesting that bulk electrical conductivity is not a prerequisite for generating the desired optical phenomena.

As we demonstrated previously, the oriented nanocomposites are potentially useful in Liquid Crystal Display applications [19]. A traditional display consists of a twisted-nematic (TN) electro-optical cell which is sandwiched between two polarisers [35]. The TN cell switches the polarisation direction of light depending on the voltage which is applied across the cell. Consequently, the two polarisers are effectively put into a parallel or perpendicular position and light is either transmitted ("off"-state) or completely absorbed ("on"-state). The nanocomposites presented in this study transmit (coloured) light for both principal polarisation directions. Therefore, a system comprised of a polariser, a TN-cell and, finally, a film with a polarisation dependent colour will transmit light in both the "on" and "off"-state which, in principal, raises the light efficiency of the device.

The main merits of the presented route towards oriented metal nanocomposites are that flexible, polymeric films are obtained without by-products originating from the reduction of metal salts. These nanocomposites can be produced using conventional processing techniques such as melt-extrusion in combination with solid-state film drawing.

Acknowledgements

The authors acknowledge the Swiss National Science Foundation and ETH Zürich (Templated Materials Project) for financial support. Early contributions of C. Darribère and W. Heffels are greatly appreciated.

References

1. F. A. COTTON and G. WILKINSON, "Anorganische Chemie" (Verlag Chemie, Weinheim, 1974) p. 1110.
2. G. SCHMID and A. LEHNERT, *Angew. Chem.* **101** (1989) 773.
3. M. BRUST, M. WALKER, D. BETHELL, D. J. SCHIFFRIN and R. WHYMAN, *J. Chem. Soc. Chem. Commun.* (1994) 801.
4. B. A. KORGEL and D. FITZMAURICE, *Adv. Mater.* **10** (1998) 661.
5. J. R. HEATH, C. M. KNOBLER and D. V. LEFF, *J. Phys. Chem. B* **101** (1997) 189.
6. K. E. GONSALVES, G. CARLSON, X. CHEN, S. K. GAYEN, R. PEREZ and M. JOSE-YACAMAN, *Nanostruct. Mater.* **7** (1996) 293.
7. K. E. GONSALVES, G. CARLSON, J. KUMAR, F. ARANDA and M. JOSE-YACAMAN, *ACS Symp. Ser.* **622** (1996) 151.
8. D. YU. GODOVSKI, *Adv. Polym. Sci.* **119** (1995) 81.
9. L. L. BEECROFT and C. K. OBER, *Chem. Mater.* **9** (1997) 1302.
10. E. J. A. POPE, M. ASAMI and J. D. MACKENZIE, *J. Mater. Res.* **4** (1989) 1018.
11. T. KYPRIANIDOU-LEODIDOU, P. MARGRAF, W. CASERI, U. W. SUTER and P. WALTHER, *Polym. Adv. Technol.* **8** (1997) 505.
12. W. MAHLER, *Inorg. Chem.* **27** (1988) 435.
13. I. A. AKIMOV, I. YU. DENISYUK and A. M. MESHKOV, *Opt. Spektrosk.* **72** (1992) 1026; Engl. Transl: *Opt. Spectrosc.* **72** (1992) 558.
14. Y. WANG and N. HERRON, *J. Phys. Chem.* **95** (1991) 525.
15. S. OGAWA, Y. HAYASHI, N. KOBAYASHI, T. TOKIZAKI, A. NAKAMURA, *Jpn. J. Appl. Phys.* **33** (1994) L331.
16. Y. WANG and W. MAHLER, *Opt. Commun.* **61** (1987) 233.
17. L. ZIMMERMANN, M. WEIBEL, W. CASERI, U. W. SUTER and P. WALTHER, *Polym. Adv. Technol.* **4** (1992) 1.
18. T. KYPRIANIDOU-LEODIDOU, W. CASERI and U. W. SUTER, *J. Phys. Chem.* **98** (1994) 8992.
19. Y. DIRIX, C. BASTIAANSEN, W. CASERI and P. SMITH, *Adv. Mater.* **11** (1999) 223.
20. C. BASTIAANSEN, H. W. SCHMIDT, T. NISHINO and P. SMITH, *Polymer* **34** (1993) 3951.
21. W. OSTWALD, "Die Welt der Vernachlässigten Dimensionen," 12th ed. (Dresden und Leipzig Verlag, 1944) p. 60.
22. J. TURKEVICH, G. GARTON and P. C. STEVENSON, *J. Colloid Sci. Suppl.* **1** (1954) 26.
23. R. ZSIGMONDY, "Kolloidchemie, 1. Allgemeiner Teil" (Otto Spamer, Leipzig, 1925) p. 43.
24. F. ZIMMERMANN and A. WOKAUN, *Mol. Phys.* **73** (1991) 959.

25. H. AMBRONN, *Kgl. Sächs. Ges. Wiss.* **8** (1896) 613.
26. H. AMBRONN and R. ZSIGMONDY, *Ber. Sächs. Ges. Wiss.* **51** (1899) 13.
27. S. BERKMAN, J. BÖHM and H. ZOCHER, *Z. Physik. Chem.* **124** (1926) 83.
28. A. FREY-WYSSLING, *Protoplasma* **27** (1937) 372.
29. *Idem., ibid.* **27** (1937) 563.
30. E. H. LAND and C. D. WEST, in "Colloid Chemistry," edited by J. Alexander (Reinhold, New York, 1946) p. 170.
31. E. H. LAND, *J. Opt. Soc. Amer.* **41** (1952) 957.
32. C. A. FOSS JR., G. L. HORNYAK, J. A. STOCKERT and C. R. MARTIN, *Mater. Res. Soc. Symp. Proc.* **286** (1992) 431.
33. N. A. F. AL-RAWASHDEH, M. L. SANDROCK, C. J. SEUGLING and C. A. FOSS, *J. Phys. Chem. B.* **102** (1998) 361.
34. A. H. LU, G. H. LU, A. M. KESSINGER and C. A. FOSS, *ibid.* **101** (1997) 9139.
35. M. SCHADT and W. HELFRICH, *Appl. Phys. Lett.* **18** (1971) 127.

Received 27 October
and accepted 18 November 1998